IN-ROLL STRESS ANALYSIS OF WOUND ROLL WITH THE AIR ENTRAINMENT AND THE PERMEATION

by

K. Tanimoto,
Mitsubishi Heavy Industries
JAPAN

ABSTRACT

The quality of a wound roll is highly dependent upon the in-roll stress distribution, which is controlled by the operating parameters of center torque, nip and tension. With increasing demands for higher performance of paper winding machines in terms of higher speed of winding, wider width of web and larger diameter of wound rolls, it becomes of vital importance to determine the optimum operating conditions of the machines.

In this paper, a numerical formulation for estimating the in-roll stress of a wound roll is proposed taking account of the effect of nonlinearity in web compressibility, air-entrainment and permeance. The proposed theory of winding is based on the assumption that the accumulation of the in-roll stress by a wound-in layer can be expressed as the superposition of the stress increments calculated from a mechanical model of a pressured thick cylinder. The theory of elasto-hydrodynamic lubrication with the compressibility of air is introduced to evaluate the effect of air-entrainment at the roll-inlet. Permeance of air is newly incorporated into the winding model, which is expressed under the assumption that permeance is proportional to the pressure difference of both sides of a web.

Winding tests were conducted in order to assure the applicability of the proposed theory by usage of the dry-end section of the paper-making pilot machine under the operating conditions of 200 ~ 2000m/min in winding speed, 765mm in web width and 1200mm in diameter of the wound roll. The numerical analysis and experimental observation shows the significant effect of the air-entrainment and permeance upon the in-roll stress.

NOMENCLATURE

$\sigma_j(i)$, $\Delta\sigma_j(i)$ Stress and stress increment of j-th layer in the winding of i-th layer

r, r_{out}	Radial position in a wound roll and outer-most radius
σ_r, σ_t	Radial and circumferential stress
ε_r, ε_t	Radial and circumferential strain
E_r, E_t	Radial and circumferential elastic modulus
ν_{rt}, ν_{tr}	Poisson's ratio
E_c	Core stiffness
T_w, T_{in} and T_{wit}	Original web tension, tension at the nip-inlet, and wound-in tension
μ_{pdi}	Coefficient of friction between the web and the nip roll
θ	Rap angle on the nip roll
α_{tq}	Share ratio of roll-torque (see equation {7})
μ_{pp}	Effective coefficient of friction between web layers
N	Nip load per unit length in the axial direction
R_q	Equivalent root mean square roughness
p	Air pressure
h	Air-film thickness
μ_q	Viscosity of air
U	Winding speed
ΔN_j	The number of "pseudo" air molecules which move toward the radial direction through a web of radius r_j per unit area in the period of Δt_i
P_j, P_a	Absolute air pressure of j-th layer and ambient pressure
α_j	Coefficient of permeance of a web per unit period and unit pressure difference

INTRODUCTION

Web is widely finished as wound for efficiency of transportation and storage in the paper or film making and finishing industry. A reel or winder is usually located at the end of the dry-end section and is one of the most important parts to control the quality of the final products.

With the increasing demands for higher performance of paper winding machines, it is getting more delicate to maintain the stable and optimum winding operations. For example, high-speed winding of coated paper sometimes causes roll defects of lateral slide or wrinkle due to the air-entrainment in the wound roll.

In order to cope with such difficulties, in-roll stress fields of wound rolls have been investigated experimentally and theoretically by many precursors to clarify the influences of winding parameters. Altmann's [1] or Hakiel's [2] theories are well known as the basic winding model and widely used academically and practically. These numerical models have been assured and modified by many researchers. Authors [3] also extended the Hakiel's model and made an examination of the conditions to cause wrinkles or breakage in wound rolls. This examination showed, however, that our theories had some restrictions of their applicability to a much porous web or to the low-speed winding. The evaluation of the air-entrainment in the wound roll was found to be indispensable to investigate the roll quality for recent high-speed winding of less porous web, e.g., coated paper or film because entrained air is stored inside the roll to change the roll structure due to its low permeability [4].

In this paper, a numerical formulation for estimating the in-roll stress of wound roll is developed taking account of the effect of air-entrainment and permeance. The theory of elasto-hydrodynamic lubrication is introduced to evaluate the effect of air-entrainment

at the roll-inlet. Permeance of air is evaluated to be proportional to the pressure difference of both sides of a web. Winding tests were conducted in order to assure the applicability of the proposed theory.

THEOREM

Background and outline

Parameters in winding are shown in Fig. 1. Web is usually wound being indented by the nip roll and web tension is loaded by the roll-torque. Under the high-speed winding, wound roll becomes constructed by the combination of web layer and air layer, which is entrained from the inlet of wound roll. Radial movement of air layer in the wound roll occurs due to the gradient of radial stress when a web has permeability.

Numerical analysis of winding was originated from using isotropic linear winding model for the estimation of the in-roll stress of wound textile or magnetic tape. Altmann [1] had extended them into anisotropic one. Hakiel [2] made a further extension to anisotropic nonlinear one by introducing incremental analysis using finite difference technique.

The numerical evaluation of air-entrainment was derived from the theories for foil bearing. Chang [5] had applied it to the winding model to demonstrate the significant effect of winding speed, nip load and stiffness of wound roll.

Parameters to be considered in our theoretical treatment are shown in Fig. 2. Our theoretical analysis is based on the Hakiel's model. Wound-in tension is estimated by introducing the effective coefficient of friction [6, 7] under the nip region. Air-entrainment is evaluated by extending Chang's theory to be able to take into account of web tension. The effect of permeance is newly incorporated into winding model.

Governing equations of winding

The schematic figure of the superposition of in-roll stress in winding is shown in Fig. 3. The stress increment of the j-th layer in winding of the i-th layer is described as the change in stress when circumferential stress which corresponds to the wound-in tension is applied to the stress-free cylinder. Total in-roll stress is acquired by summing up these stress increments shown in equation {1}.

$$\sigma_j(i) = \sigma_j(i-1) + \Delta\sigma_j(i) \qquad \{1\}$$

Equiribrium equation, compatibility equation and stress-strain relations are shown in equations {2.1}~{2.3}.

$$r\frac{d\sigma_r}{dr} + \sigma_r - \sigma_t = 0 \qquad \{2.1\}$$

$$r\frac{d\varepsilon_t}{dr} + \varepsilon_t - \varepsilon_r = 0 \qquad \{2.2\}$$

$$\varepsilon_r = \frac{\sigma_r}{E_r} - \nu_{rt}\frac{\sigma_t}{E_t}, \quad \varepsilon_t = \frac{\sigma_t}{E_t} - \nu_{tr}\frac{\sigma_r}{E_r} \qquad \{2.3\}$$

Combination of these equations leads to the second order differential governing equation {3}.

$$r^2\frac{d^2\sigma_r}{dr^2}+(3+\nu_{rt}-\frac{E_t}{E_r}\nu_{tr})r\frac{d\sigma_r}{dr}+(1-\frac{E_t}{E_r}+\nu_{rt}-\frac{E_t}{E_r}\nu_{tr})\sigma_r=0 \qquad \{3\}$$

The equation {1} and equation {3} can be combined into equation {4} concerning about the radial stress increment $\Delta\sigma_r$, where subscript j is excluded for simplicity.

$$r^2\frac{d^2\Delta\sigma_r}{dr^2}+(3+\nu_{rt})r\frac{d\Delta\sigma_r}{dr}+(1-\frac{E_t}{E_r}+\nu_{rt})\Delta\sigma_r=0 \qquad \{4\}$$

Inner and outer boundary conditions are as follows.

(i) Inner boundary condition : Equiribrium of the radial stress increment and circumferential strain increment

$$E_c=\left.\frac{\Delta\sigma_r}{\Delta\varepsilon_t}\right|_{r=r_c} \qquad \{5\}$$

(ii) Outer boundary condition : Equiribrium of the radial stress increment and the pressure increment correspond to the wound-in tension

$$\Delta\sigma_r\Big|_{r=r_{out}}=-\left.\frac{T_{wit}}{r}\right|_{r=r_{out}} \qquad \{6\}$$

Wound-in tension

Wound-in tension is no longer equal to the original web tension T_w due to the following two reasons.

(i) Change in tension on the nip roll

Cai [8] explained that tension will be lost due to the micro-slip on the nip roll especially in surface winding according to the Euler's theorem. When both the nip roll and the wound roll are driven, authors [3] described the tension at the nip-inlet T_{in} under the assumption that T_{in} changes proportionally according to the share ratio of roll-torque α_{tq}, as in the following.

$$T_{in}=\alpha_{tq}T_w+(1-\alpha_{tq})\frac{T_w}{\exp(\mu_{pd}\theta)} \qquad \{7\}$$

(ii) Change in tension when passing the nip region

Pfeiffer [9] and Good [10] made the experimental and theoretical examination about the change in tension when passing the nip region. They concluded that this change in stress is caused by the interlayer slip just below the nip roll, especially by the slip of outer-most few layers and Good expressed this change in tension, that is, nip-induced tension T_{nit} as equation {8}.

$$T_{nit} = \mu_{pp} N \quad \{8\}$$

With the increasing winding speed, the contact condition at the nip region transits from boundary lubrication to fluid lubrication, which will reduce friction. We introduce Good's [6] proposition that "effective" coefficient of friction between web layers μ_{pp} has the relationship with the equivalent root mean square roughness R_q. We obtain equation {9} from the combination of equations {7} and {8}.

$$T_{wot} = T_{in} + T_{nit} = \alpha_{tq} T_w + \frac{(1-\alpha_{tq})T_w}{\exp(\mu_{pd}\theta)} + \mu_{pp} N \quad \{9\}$$

Estimation of air-entrainment

Air-film thickness is evaluated using solution of the elasto-hydrodynamic lubrication for foil bearing. The governing equation shown below is Reynold's equation considering the compressibility of air.

$$f_1 = \nabla \cdot (ph^3 \nabla p) - 6\mu_a U \frac{\partial (ph)}{\partial x} = 0 \quad \{10\}$$

Equiribrium equation with the nip load is shown in equation {11}.

$$f_2 = \int_A p(l_n) dA - N = 0 \quad \{11\}$$

Newton-Raphson technique can be applied to solve these equations {10} and {11}.

Equivalent elastic modulus of wound roll including air-layer

The radial elastic modulus of the wound roll with air-layer becomes much lower than that without air-layer. Good [11] introduced equivalent rigidity of the combination of the web and the air-layer.

$$E_{req} = \frac{\Delta \sigma_r}{\Delta \varepsilon_{req}} = \frac{t_o + h_o}{\frac{t_o}{E_{rf}} + \frac{h_o}{E_{rair}}} \quad \{12\}$$

The radial modulus of web E_{rf} is derived from the gradient of its stress-strain curve. Meanwhile the modulus of air-layer E_{rair} is calculated from Boyles's Law assuming that entrained air is ideal gas and that its volume changes under isothermal condition.

$$E_{rair} = \frac{(|\sigma_r| + p_a)^2}{p_o + p_a} \quad \{13\}$$

Where p_o is the pressure inside the outer-most layer when it was wound. Considering equation {13}, the radial modulus in the governing equation {3} E_r is replaced by equivalent radial modulus E_{req}.

Stress change due to permeance

The entrained air moves toward the radial direction through a web layer when a web has the permeability. Stress change due to the permeance is expressed by the two governing relationships. One is the equation of the permeance, which is derived from the assumption that the air-permeance is proportional to the pressure difference of both sides of the web. The other is the equiribrium equation of the web supported by its tension and pressure of both sides. Fig. 4 showed the model of the permeance. Now we consider the stress change in the period of Δt_i , which is the interval from the time when the (i-1) -th layer is wound to the time when the i-th layer is wound. ΔN_j is defined as the number of the "pseudo" air molecule which moves toward the radial direction through a web of radius r_j per unit area in the period of Δt_i .

Assuming that the entrained air is ideal gas, we obtain the following equation of state concerning the j-th layer, using absolute pressure P_j, volume V_j, the number of the pseudo air molecule No_j and absolute temperature T.

$$P_j V_j = No_j KT \qquad \{14\}$$

Absolute pressure P_j is equal to $-\sigma_r$ plus ambient pressure P_a.

$$P_j = -\sigma_r + P_a \qquad \{15\}$$

Volume V_j is expressed using radial position r_j and thickness of air layer h_j as follows.

$$V_j = 2\pi r_j h_j \qquad \{16\}$$

The number of the change of the pseudo air molecule ΔNo_j is defined as the difference between the number of the pseudo air molecule which flow in from the surface of r_j to the j-th layer, ΔN_j, and that which flow out from the surface of r_{j+1}, ΔN_{j+1}.

$$\Delta No_j = 2\pi(r_j \Delta N_j - r_{j+1}\Delta N_{j+1}) \qquad \{17\}$$

ΔN_j is evaluated using the pressure difference of both sides of j-th layer as in the following.

$$\Delta N_j = \frac{dN_j}{dt}\Delta t = \alpha_j \Delta t(P_{j-1} - P_j) \qquad \{18\}$$

Coefficient of permeance per unit period and unit pressure difference, α_j, is given from the test of Gurley air resistance [12].

Next, we consider the equiribrium equation of the web. Fig. 5 shows the coordinates and external forces applied to the j-th layer. The web layer is supported by its tension and pressure of both sides. We can obtain the following equiribrium equation and the compatibility equation.

$$\sigma_{t,j} t_j d\theta + P_{j+1} r_{j+1} d\theta = P_j r_j d\theta + P_j h_j d\theta \qquad \{19\}$$

$$r_{j+1} = r_j + (t_j + h_j) \quad \{20\}$$

The change in circumferential stress $\Delta\sigma_{t,j}$ due to the change in radial position r_j is derived from Hook's Law.

$$\Delta\sigma_{t,j} = E_t \frac{\Delta r_j}{r_j} \quad \{21\}$$

Equations $\{14\} \sim \{21\}$, converted into incremental expressions, can be solved simultaneously to obtain the change of pressure ΔP_j due to the permeance.

Numerical procedure

Fig. 6 shows the flow of the in-roll stress analysis of the wound roll. Several pairs of the air layer and the web layer can be regarded as one "equivalent" layer as long as the numerical precision is maintained.

EXPERIMENTAL VERIFICATIONS

Experimental procedure

Experimental investigations were performed to assure the applicability of the numerical winding model. Winding tests were conducted by usage of the dry-end section of our paper-making pilot machine. Fig. 7 shows the schematic figure of our testing machine. New wound roll is placed at the wound-off and the web is drawn out under the preset speed by the drag roll. Winding tension is applied by the prescribed torque of both the nip roll and wound roll. Interlayer pressure $-\sigma_r$ is measured using pull-tabs and FlexiForce™. The former is a thin steel plate of 0.05mm thick and the load to be pulled is measured. The latter is a sensor that senses the change in resistance caused by the pressure in the wound roll. Both are calibrated beforehand by putting them in the stack of the same grade of paper and being loaded using the universal testing machine. These pull-tabs and FlexiForce™ are inserted in the paper sleeve and are pasted at the both edge of the web in advance.

Test conditions

Material properties and winding parameters are listed on the Table 1 and Table 2. The major operating conditions of 200 ~ 2000m/min in winding speed, 765mm in web width and 1200mm in maximum diameter of the wound roll are selected. Two kinds of coated papers with the different Gurley air resistance are prepared. The torque applied to the wound roll, center torque, is expressed by converting it to the tangential load per unit width.

Numerical procedures

Three types of calculations were performed to demonstrate the effect of air-entrainment and permeance, (i) Without air, (ii) With air-entrainment and (iii) With air-entrainment and permeance.

Effect of numerical procedures

Fig. 8 shows the radial stress $-\sigma_r$ of three types of calculations (i), (ii) and (iii) of

paper A with the winding speed of 800m/min and the nip load of 2.2kN/m. The mean values of the experimental data are shown with their maximum and minimum values indicated by the error bars. Absolute value of radial stress in calculation (ii) is evaluated as about half of calculation (i) because of the consideration of air-entrainment. This is because lowered equivalent radial stiffness due to entrained air layer makes its anisotropy much higher, which prevents the accumulation of radial stress increment of its inner part. Air-permeance reduces the air thickness of inside of the wound roll to cause the absolute value of radial stress higher. On the other hand, air-permeance also reduces the radius of a web layer to loosen its circumferential stress, which makes the absolute value of radial stress lower. In the above calculations, the effect of the former one is found to be much more significant.

Theoretical results of calculation (iii), which includes the effect of air-entrainment and permeance, agree best with the experimental ones.

Effect of winding parameters

Fig. 9 shows the comparison of theoretical and experimental results of radial stress $-\sigma_r$ for various parameters to be surveyed. Calculation (iii) is selected.

Fig. 9(a) shows the effect of the winding speed of paper B with the nip load of 2.2kN/m. The winding speed of 2000m/min is achieved from the radius of 400mm. Higher speed makes the absolute value of radial stress lower. As mentioned before, higher winding speed increases the entrained air to reduce its radial stiffness. Comparing with the experimental ones, the inclination to become lower in the absolute value of radial stress with the increasing speed is expressed, however, quantitative agreements are unsatisfactory, especially at the lower speed. This may be caused by the underestimation of air-entrainmet at the lower speed.

Fig. 9(b) shows the effect of the nip load of paper A with the winding speed of 800m/min. Higher nip load makes the absolute value of radial stress higher. These phenomena coincide with the results reported by many researchers. In these cases, effectiveness of coefficient of friction to evaluate the nip-induced tension is less than 30%, which is estimated by the comparison between the entrained air layer thickness and surface roughness. Sufficient agreements with the experimental ones are observed.

Fig. 9(c) shows the effect of paper grade with the winding speed of 500m/min and the nip load of 2.2kN/m. Lower permeability of paper makes the absolute value of radial stress lower qualitatively, however, little influence is observed. In this test condition, winding speed is so slow that most of entrained air is permeated.

CONCLUSIONS

We proposed a new theoretical formulation for paper winding taking account of nonlinearity in paper compressibility, air-entrainment and permeance. The in-roll stress fields were examined theoretically and experimentally and they showed the significant effect of the air-entrainment and permeance upon the in-roll stress.

REFERENCES

1 Altmann, H. C., "Formulas for Computing the Stresses in Center-Wound Rolls", Tappi Journal, Vol.51 No.4, 1968, pp.176-179.

2 Hakiel, Z., "Nonlinear Model for Wound Roll Stresses", Tappi Journal, Vol.70 No.5, 1987, pp.113-117.

3 Tanimoto, K., Kohno, K., Yamamoto, M. and Watanabe, T., "Numerical

Simulation of Wound Roll", 1996 JAPAN TAPPI Annual Meeting Proceedings, JAPAN TAPPI, Toyama, 1996.
4 Tanimoto, K., Kohno, K., Takahashi, S., Sasaki, M. and Yoshida, F., "Numerical Stress Analysis of Wound Roll with Air-entrainment", Transactions of the Japan Society of Mechanical Engineers, In printing (2001).
5 Chang, Y. B., Chambers, F. W., and Shelton, J. J., "Elastohydrodynamic Lubrication of Air-Lubricated Rollers", ASME Journal of Tribology, Vol.118, 1996, pp.623-628.
6 Good, J. K., Kedl, D. M., and Shelton, J. J., "Shear Wrinkling in Isolated Spans", Proceedings of the Fourth International Conference on Web Handling, Web Handling Research Center, Stillwater, Oklahoma, 1997, pp.462-479.
7 Hashimoto, H., "Tribological Approach to Web Handling Problems", Proceedings of the Japan Society of Mechanical Engineers, Vol.1999 No.5, 1999, pp.183-184.
8 Cai, N., "The Effect of Nip Roll Compliancy upon Center and Surface Winding", Oklahoma State Univ. M. S. Thesis, 1992.
9 Pfeiffer, J. D., "Nip Forces and Their Effect on Wound-in Tension", Tappi Journal, Vol.60 No.2, 1977, pp.115-117.
10 Good, J. K. and Wu, Z., "The Mechanism of Nip-Induced Tension in Wound Rolls", Transaction of ASME, Journal of Applied Mechanics, Vol.60, 1993, pp.942-947.
11 Good, J. K., and Covell, S. M., "Air Entrapment and Residual Stresses in Rolls Wound With a Rider Roll", Proceedings of the Third International Conference on Web Handling, Web Handling Research Center, Stillwater, Oklahoma, 1995, pp.95-111.
12 TAPPI, "1998-1999 TAPPI TEST METHODS", T460 om-96, TAPPI PRES, 1998.

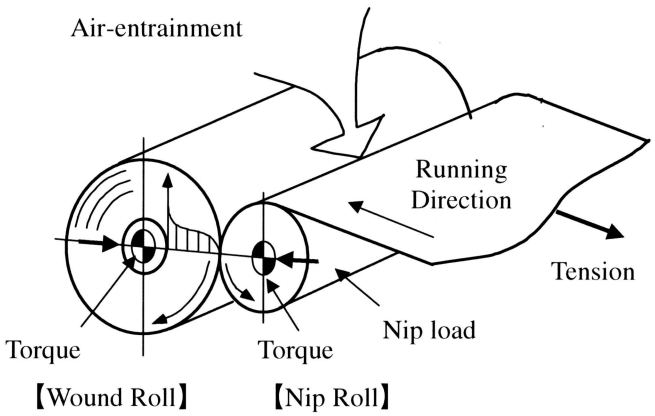

Fig. 1 Parameters in winding

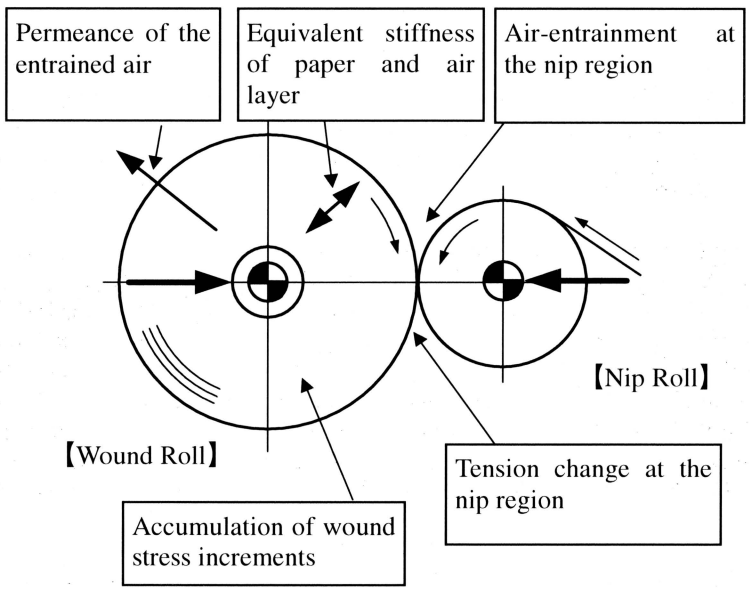

Fig. 2 Parameters to be considered in theoretical treatment

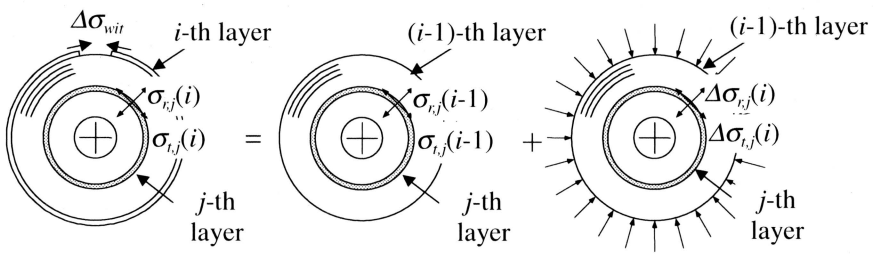

Fig. 3 Superposition of incremental stress

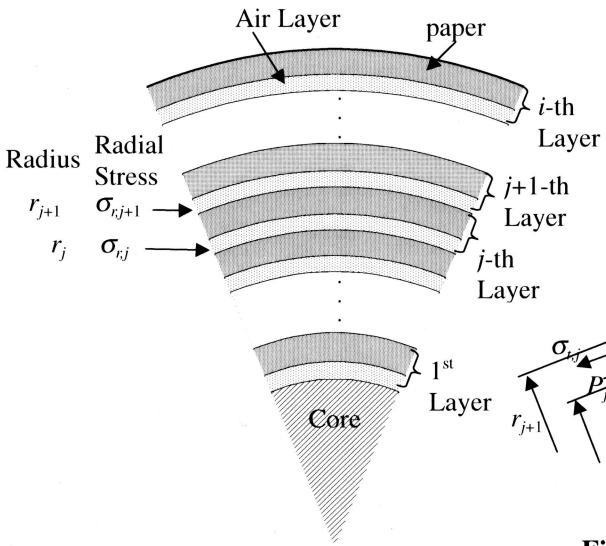

Fig. 4 Model of Permeance

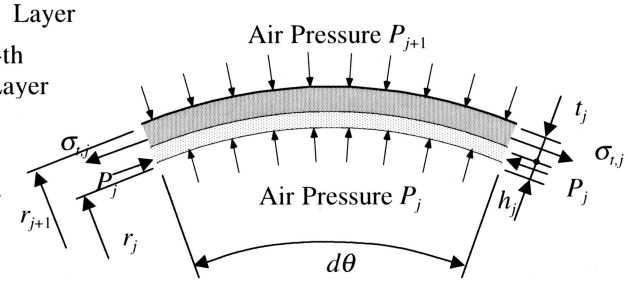

Fig. 5 Coordinates and external forces applied to a layer

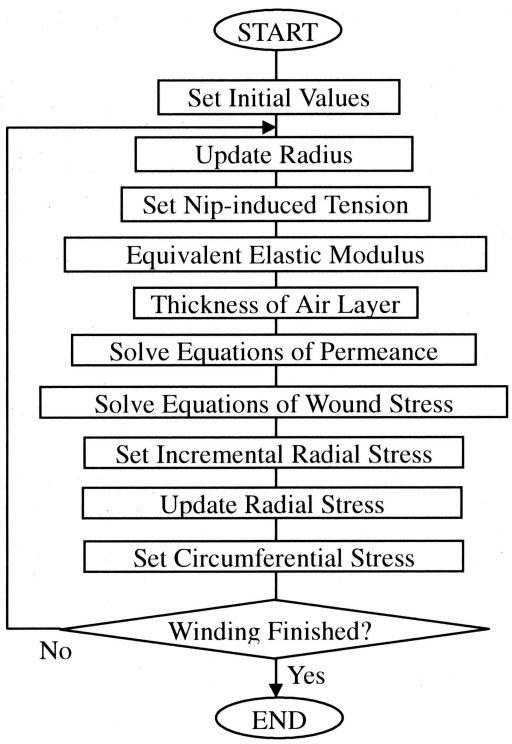

Fig. 6 Flow of calculation

Table 1 Material properties

Item		Value	
Paper Grade		Paper A	Paper B
Thickness t (mm)		0.0605	0.0460
Air Resistance of Paper (Gurley method) β (sec)		10400	3160
Stress-Strain Relation of Paper in Radial Direction $\sigma = A\varepsilon^n$ (MPa)		$A=5.42\times10^5$ n=5.00	$A=4.24\times10^3$ n=3.85
Elastic Modulus in Circumferential Direction E_t (MPa)		9873	9067
Coefficient of Friction	Paper / Paper μ_{pp}	0.344	0.320
	Paper / Nip Roll μ_{pd}	0.424	0.422
Poisson's Ratio	ν_{rt}	0	
	ν_{tr}	0.3	
Core Stiffness E_c (MPa)		2.57×10^4	

Table 2 Winding parameters

Paper Grade	Speed V (m/min)	Nip Load N (kN/m)	Tension T_w (kN/m)	Center Torque T_q (kN/m)
Paper A	500～1000	1.6～2.2	0.4	0.25～0.35
Paper B	200～2000	2.2		0

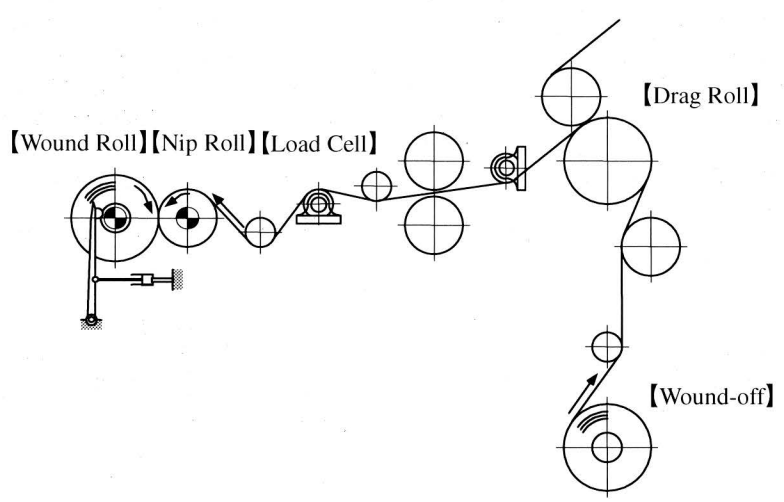

Fig. 7 Testing machine

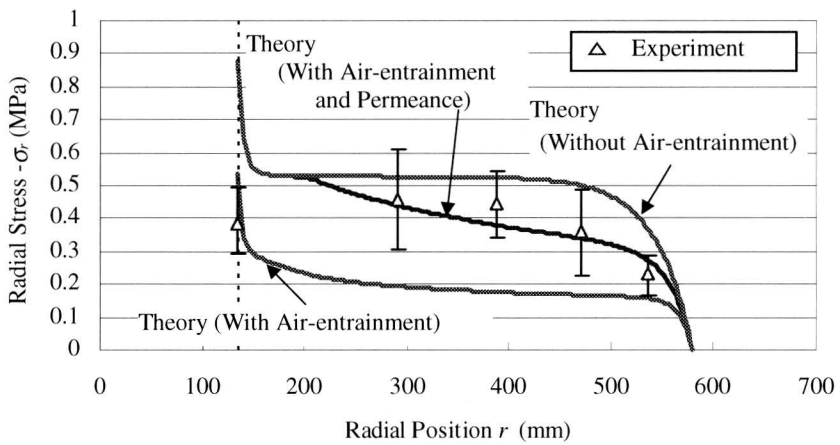

Fig. 8 Theoretical and Experimental Results
- Effect of Theoretical Method -

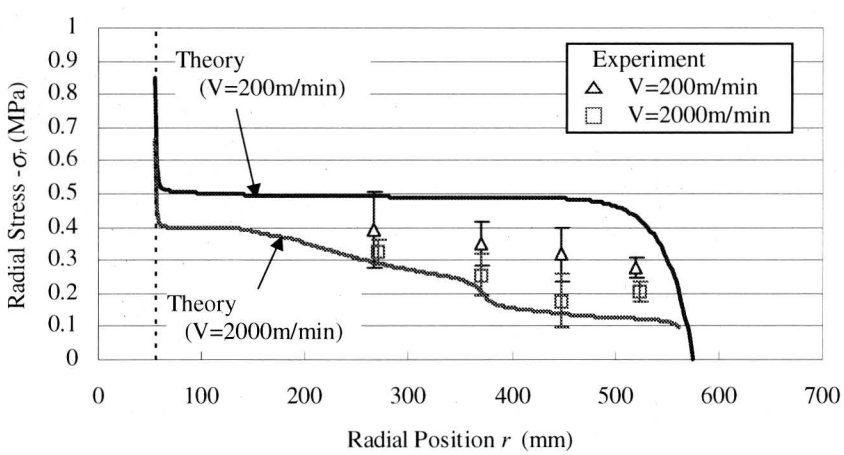

(a) Effect of Winding Speed
Fig. 9 Theoretical and Experimental Results

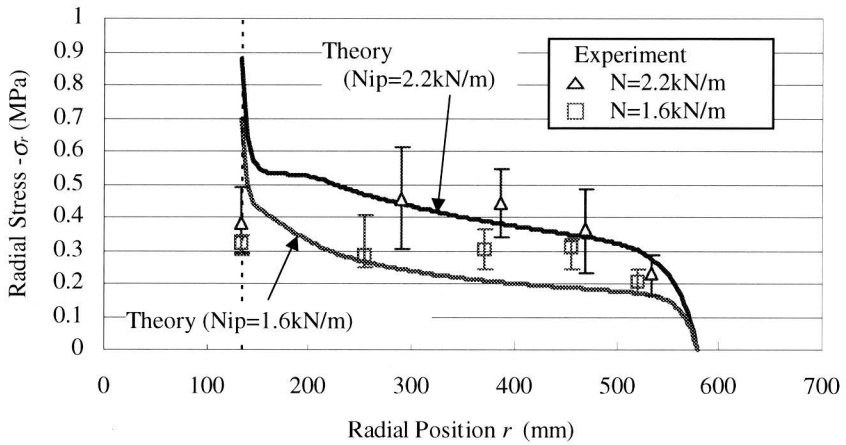

(b) Effect of Nip Load

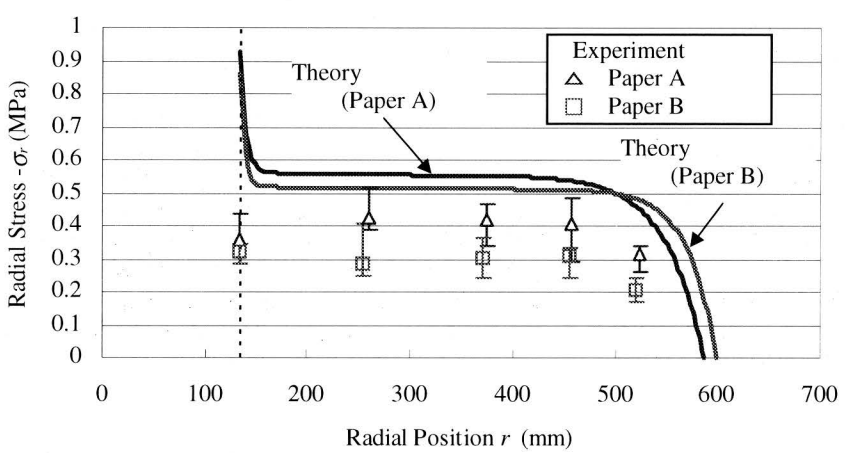

(c) Effect of Paper Grade

Fig. 9 Theoretical and Experimental Results

Name & Affiliation	**Question**
H. Lei – Eastman Kodak	At a winding speed of 2000 meters per minute, how did you put the pull tabs into the roll?
Name & Affiliation	**Answer**
K. Tanimoto – Mitsubishi	We conducted several tests using pull tabs and the Flexiforce sensors at speeds less than 800 meters per minute. The test results were comparable to the results of the model. For the measurement at 2000 meters per minute, we only used the Flexiforce sensors. These sensors are light and similar to the OHP sheet and it was successful.
Name & Affiliation	**Question**
M. Jorkama – Metso Paper	You had some equations for nip-induced tension, can you explain that in more detail? I'm interested in the last two terms. What does the coefficient α represent?
Name & Affiliation	**Answer**
K. Tanimoto – Mitsubishi	When surface winding, the nip roll is driven, and the web tension will be lost due to the micro-slip. In center winding this term is equal to the web tension T_W. In winders where both center and surface torque are applied, we assume this term is proportional to the share ratio of torque.
Name & Affiliation	**Question**
K. Good – OSU	Would α be zero for surface winding and one for center winding?
Name & Affiliation	**Answer**
K. Tanimoto – Mitsubishi	Yes.
Name & Affiliation	**Question**
David Lanstrum – Quadtech International	We're involved in the printing business. You mentioned a Paper A and Paper B, one of which was coated. Could you specifically mention what type of coating?
Name & Affiliation	**Answer**
K. Tanimoto – Mitsubishi	We used 3 kinds of paper. Two were coated papers and 1 was newsprint.
Name & Affiliation	**Question**
David Landskron – Quad Tech International	What types of coating were used? Were they clay or plastic
Name & Affiliation	**Answer**
K. Tanimoto – Mitsubishi	They were clay based.
Name & Affiliation	**Question**
R. Lucas – GL&V	On your slide in which you showed the radial stiffness with permeance; how much time transpired before you made your measurements and would a different time delay

	effect the results? If you made your measurements right after you wound the roll, versus waiting an hour or a day, would it make any difference in your results?
Name & Affiliation	**Answer**
K. Tanimoto – Mitsubishi	We measured just after winding and didn't measure again.
Name & Affiliation	**Question**
R. Lucas – GL&V	Wouldn't you expect that that would change as a function of time?
Name & Affiliation	**Answer**
K. Tanimoto – Mitsubishi	Yes. Our theoretical calculation yielded results just after winding and so we conducted the tests immediately after winding.